23-2-2003

Investigating Localized Degradation of Organic Coatings

L. V. Philippe
University of Machester, UK

G. W. Walter
University of Wollongong

S. B. Lyon
University of Manchester, UK

Journal of The Electrochemical Society, **150** (4) B111-B119 (2003)
0013-4651/2003/150(4)/B111/9/$7.00 © The Electrochemical Society, Inc.

Investigating Localized Degradation of Organic Coatings

Comparison of Electrochemical Impedance Spectroscopy with Local Electrochemical Impedance Spectroscopy

L. V. S. Philippe,[a] G. W. Walter,[b] and S. B. Lyon[a,z]

[a]*Corrosion & Protection Centre, University of Manchester Institute of Science and Technology, Manchester, M60 1QD, United Kingdom*
[b]*University of Wollongong, Faculty of Engineering Materials, New South Wales, Australia*

The degradation of polyester coil-coated galvanized steel was compared using both conventional (macroscopic) and localized electrochemical impedance techniques on the same specimen and within a time interval (hours) much shorter than the total immersion period (days). Specimens containing a central 250 μm laser-ablated defect in the organic coating layer were immersed in a 10 mM NaCl solution for up to 30 days. The local multifrequency impedance was determined by placing a novel impedance probe, either directly above the coating defect or above an area of intact coating. In addition, single frequency impedance mapping of the specimen surface was carried out at 1 kHz and compared with optical microscopy of the surface. The results demonstrate clearly that macroscopic electrochemical impedance provides a surface-averaged measurement of the properties of the coating, plus any defects, and that where several time constants are apparent, they are not uniquely separable into physical processes. Thus, macroscopic impedance spectra convolute the separate responses of the coating and defect together. However, local electrochemical impedance can effectively separate the local properties of the organic coating from the local electrochemical behavior at a coating defect.
 [DOI: 10.1149/1.1554913]

Manuscript submitted April 24, 2002; revised manuscript received October 15, 2002. Available electronically February 25, 2003.

Organic coatings are widely used to prevent corrosion of metals in industry and as decorative finishes. To be effective, an organic coating should act as a good ionic and electronic barrier to the environment and/or contain an active inhibition system.[1] However, because no coating is perfect, corrosion tends to initiate at the areas of lowest ionic resistance. Such areas can be, *e.g.*, localized at cut edges on metallic structures or at intrinsically defective areas on the surface.

Once the corrosion is initiated at a defect, it can spread very quickly, leading to the delamination of the paint: water absorption and diffusion leading to a loss of coating adhesion when it reaches the coating/substrate interface. The degree to which permeated water changes the adhesion properties of the coated system is often referred to as its wet adhesion.[2,3] Once the water volume under the coating increases, a mechanical stress is created, which leads to an increase of the nonadherent surface. All the conditions, such as the availability of the species (water, oxygen, etc.), for corrosion reactions and hydrodynamic delamination due to osmotic pressures, are met for corrosion initiation. An overview of the different corrosion phenomena on polymer-coated metals can be found in Leidheiser's review.[4]

Coated systems normally corrode along the polymer/metal interface. Many models have been proposed in the literature to explain this. However, the two definitive models are cathodic delamination[5-7] and anodic undermining.[8,9] These two mechanisms can coexist, and in one system, for example, both mechanisms may occur at the same time or at different times depending on the composition of the environment and the progress of the disbonding front. This suggests that the mechanism of coating disbondment is complex and depends on the metallic substrate, the composition of its passive layer and corrosion products, and on transport phenomena.[10]

Despite many years of research, study of the localized degradation around a coating defect remains difficult mainly because this process is localized. Electrochemical impedance spectroscopy (EIS), which has been proved a very effective tool for the study of paint properties on metal substrates,[11] fails to provide information about the local electrochemical mechanisms involved in localized corrosion processes. However, because EIS provides valuable information about the quality of a coating,[12] there is considerable interest in discovering the causes of local coating breakdown; therefore, a better understanding of the surface phenomena is needed. These phenomena include parameters such as physical and chemical properties of the coating itself, the behavior of the corrosion process and its nature, and the form of localized corrosion.

Local electrochemical impedance spectroscopy (LEIS) is a recent technique[13-15] that has the potential to provide this required information and therefore is complementary to EIS. In the past few years, previous studies were carried out to develop viable LEIS techniques. Much work has focused on the improvement of the technique itself,[16] such as the design of the microreference electrodes and the way of measuring the local impedance to improve the sensitivity and the spatial resolution of the technique. In parallel, LEIS has been tested successfully on different materials for a large range of applications.[17,18]

The present study presents a comparison between conventional macroscopic EIS and LEIS. We show that EIS produces a surface-averaged measurement, which is not relevant if the interest is to focus on local corrosion phenomena, whereas LEIS can give extra information about the corrosion process and its nature in a localized manner. Surface impedance mapping at a single frequency gives further information, such as the location of defects responsible for localized corrosion.

Principles of LEIS

LEIS measurements, which may be performed under potentiostatic or galvanostatic control, are determined from the ratio of the local electrochemical potential of the substrate to the local flow of current in the solution above the substrate. To measure these quantities, a multielectrode localized probe is used. Various geometric arrangements have been proposed; all have the key features of vertically displaced dual probes for measuring the local current flow in solution and a remote counter electrode. Many arrangements also use a remote reference electrode; however, this introduces a significant error in measurement because what is required is the local electrochemical potential. In this work, dual current sense electrodes are also used. However, the electrode closest to the substrate also functions as the reference electrode for the surface potential, thus providing a more accurate local measurement. The three-electrode impedance probe is shown in Fig. 1.

In solution, the alternating applied voltage difference, ΔV, associated with the alternating current (ac) flow is measured between the

[z] E-mail: s.b.lyon@umist.ac.uk

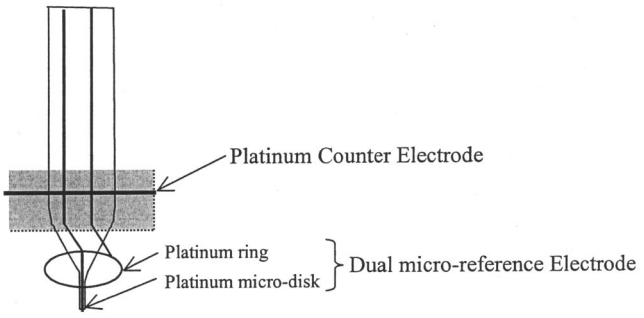

Figure 1. Schematic of the three-electrode impedance probe of the LEIS system (not in scale).

lower two probe electrodes. The local current density, i_{loc}, is then calculated

$$i_{loc} = \frac{\Delta V_{loc} K}{d} \quad [1]$$

where d is the distance between the tips of the dual probe and K is the bulk conductivity of the electrolyte. The local impedance, Z_{loc}, is then calculated directly

$$Z_{loc} = \frac{V_{loc}}{i_{loc}} \quad [2]$$

where V_{loc} is the alternating perturbation in potential of the substrate, measured at the lowest electrode (*i.e.*, that closest to the surface), because of the applied ac signal.

The preceding treatment does not take into account the height of the probe above the surface and assumes that the current density at probe height is the same as that at the surface. In reality, only a fraction of the current flows normal to the sample surface and is collected by the probe. Although this does not alter the form of the impedance plot, the absolute scale is then in error. Hence, for each particular probe design and at every height above the surface, a calibration factor for the current collection efficiency must be determined to derive the true impedance values.

Experimental

This study has been performed on industrial (coil) coated-galvanized steel with a 25 μm hot-dip zinc layer, strontium chromate pigmented epoxy primer (5-6 μm), and a polyester topcoat (25-28 μm) as working electrode. Samples were of area 3 cm^2 with a centered laser-ablated hole, of 250 μm diam (through the coating to the zinc substrate, not exposing the steel). Thus, the defect area was 0.015% of the intact coating area. All impedance measurements were performed in a 10 mM NaCl solution of conductivity 1.1 mS cm^{-1}.

The microreference electrode used for the LEIS measurements consisted of a platinum microdisk tip (diam 200 μm) and platinum ring electrode vertically separated by 3 mm (see Fig. 1). A remote platinum ring electrode was also placed vertically 3 cm above the lowest electrode. Thus, the electrochemical cell used a four-electrode system.

Impedance measurements.—Macroscopic EIS measurements used a classic three-electrode system for bulk impedance with a saturated calomel electrode as reference electrode and a platinum flag as counter electrode. A Solartron 1250 frequency response analyzer (FRA) and a Solartron 1286 potentiostat were used. The EIS frequency range was 20 kHz to 0.1 Hz with an applied ac perturbation of 20 mV rms.

LEIS measurements used a four-electrode system (shown schematically in Fig. 2) where the platinum counter electrode slides vertically above the dual-electrode probe, as stated previously. The scan head contains x,y,z direction stepping motors that allow precise positioning of the probe. The potential difference between the dual electrodes (*i.e.*, the current sense) is amplified using an electrometer set to a gain of times 10; in addition, the lower electrode of the probe is buffered at unity gain by a separate, electrically isolated

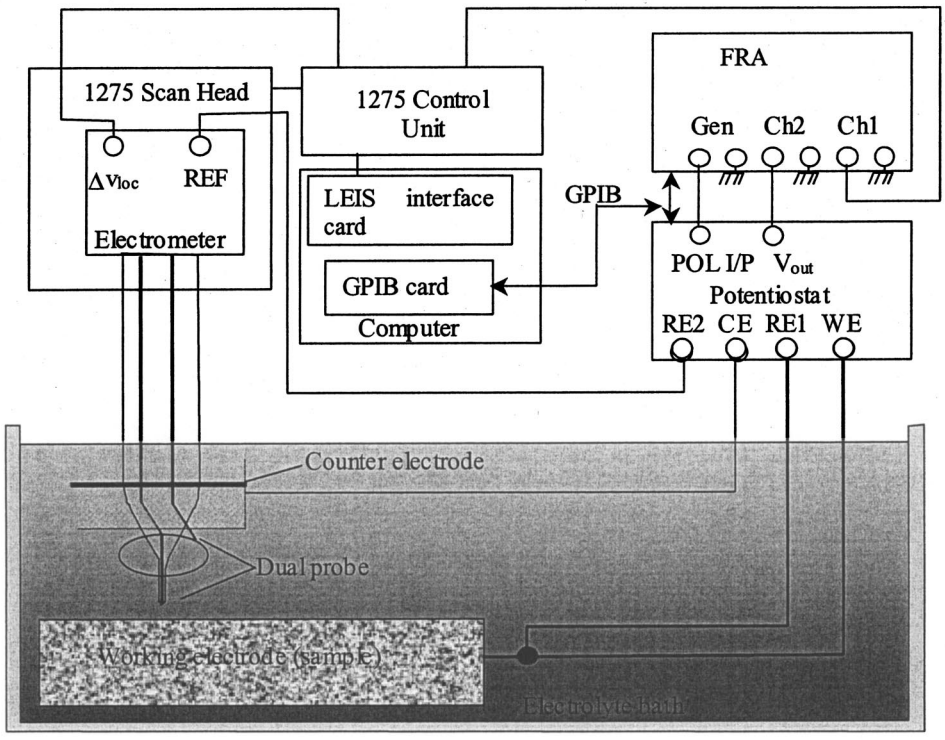

Figure 2. Schematic diagram showing the complete LEIS system, including potentiostat and FRA.

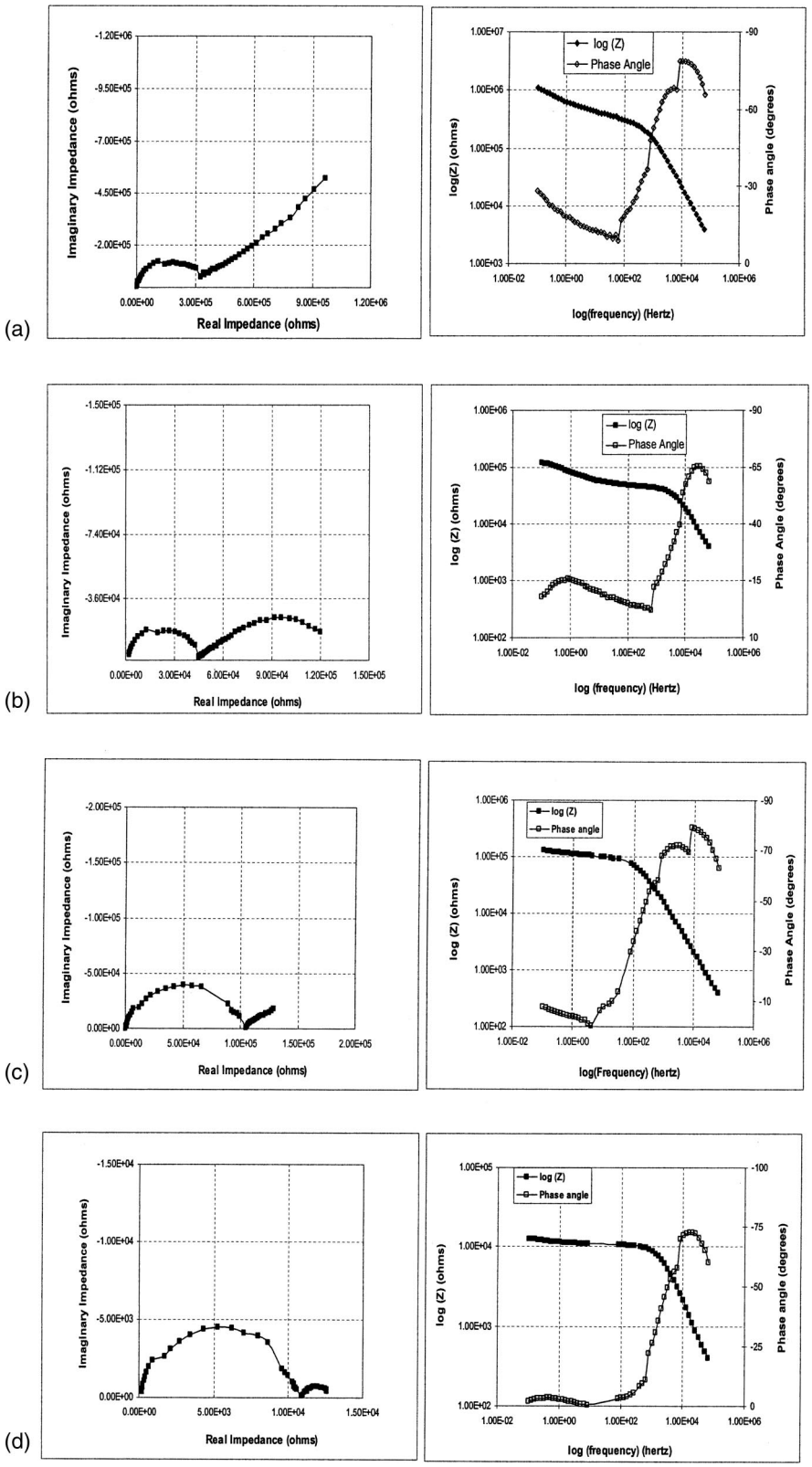

Figure 3. Nyquist and Bode plots of conventional impedance response from macroscopic specimen (polyester coil-coated galvanized steel with central 250 μm laser-ablated defect) after (a) 3 days, (b) 12 days, (c) 18 days, and (d) 30 days immersion.

electrometer. A Solartron 1250 FRA and a 1286 potentiostat were used in conjunction with a Uniscan Instruments x,y,z positioning system (1275). The 1286 controls the sample potential using the lower electrode on the probe as a reference. For potentiostatic measurements, a single ended input, working electrode earthed, electrometer amplifier module is used, and the system may be controlled at any desired potential with the 1250 recording ac voltage and current measurements for calculation of impedance at each measurement point. For measurements at the corrosion (rest) potential, an alternative dual floating input electrometer amplifier module is used, and the potentiostat is configured as a galvanostat with an appropriate current range chosen to restrict the sample potential perturbation in the range 10-20 mV rms. The frequency range used was generally 20 kHz to 0.1 Hz. However, due to the small areas of the platinum

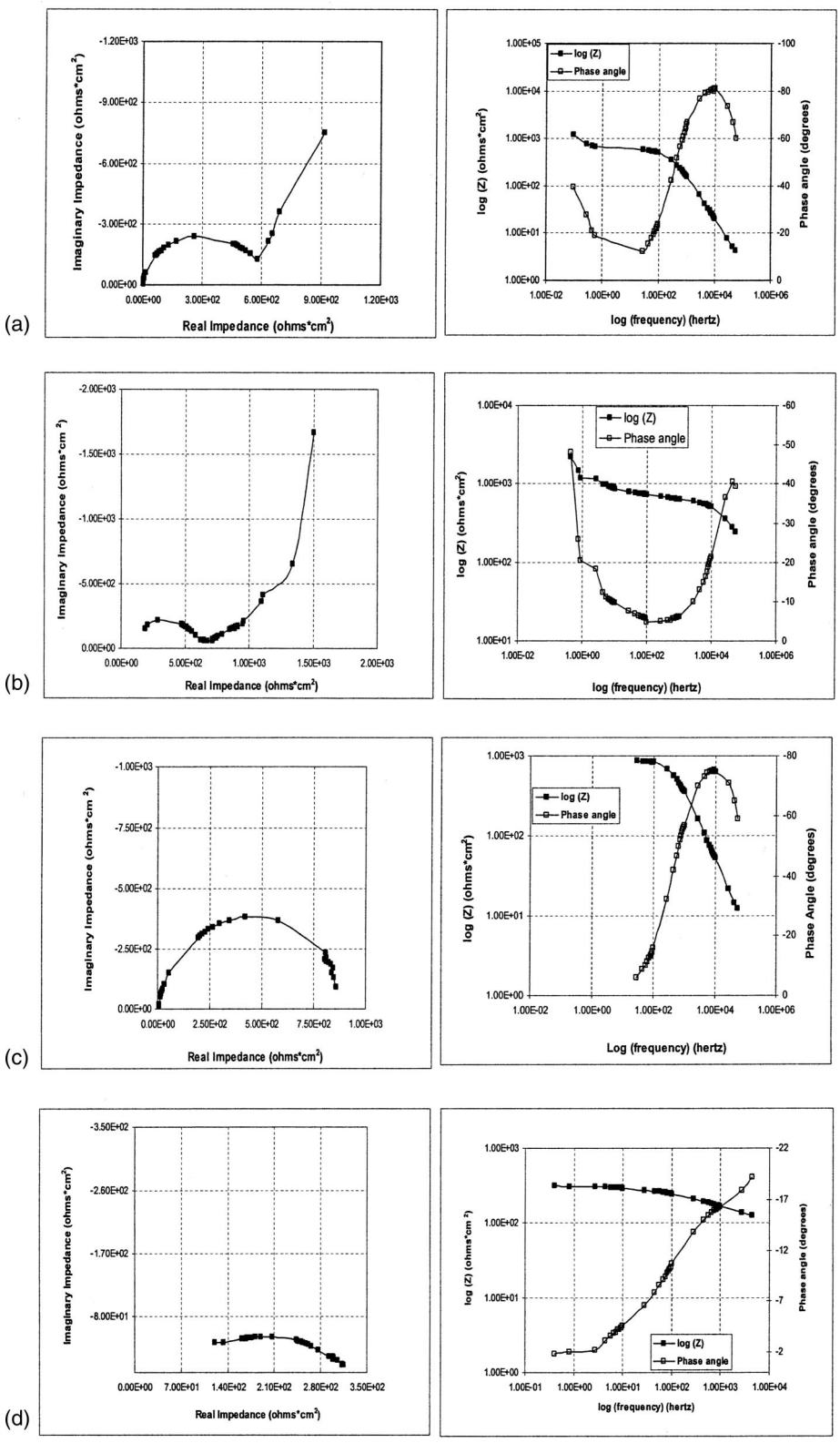

Figure 4. Nyquist and Bode plots of the LEIS response on polyester coil-coated galvanized steel directly above the coating defect after (a) 3 days, (b) 12 days, (c) 18 days, and (d) 30 days of immersion.

microelectrodes, measurements at frequencies of the order of 1 Hz or less were restricted due to noise. The Uniscan Instruments control software collects the data automatically and displays them in the form of Nyquist and Bode plots (multifrequency measurement), area maps, and line graphs (single frequency measurement).

At intervals for a total of 30 days immersion, conventional EIS measurements were carried out on the macroscopic sample including the defect. Immediately following such measurements, separate LEIS data were also obtained on the same sample directly above the defect and also above the same intact area of the coating. Thus, the time interval between the EIS and the LEIS measurements (hours) was much shorter than the total immersion period (days). Importantly, the area of intact coating from which measurements were taken was located along the diagonal of the square exposed sample

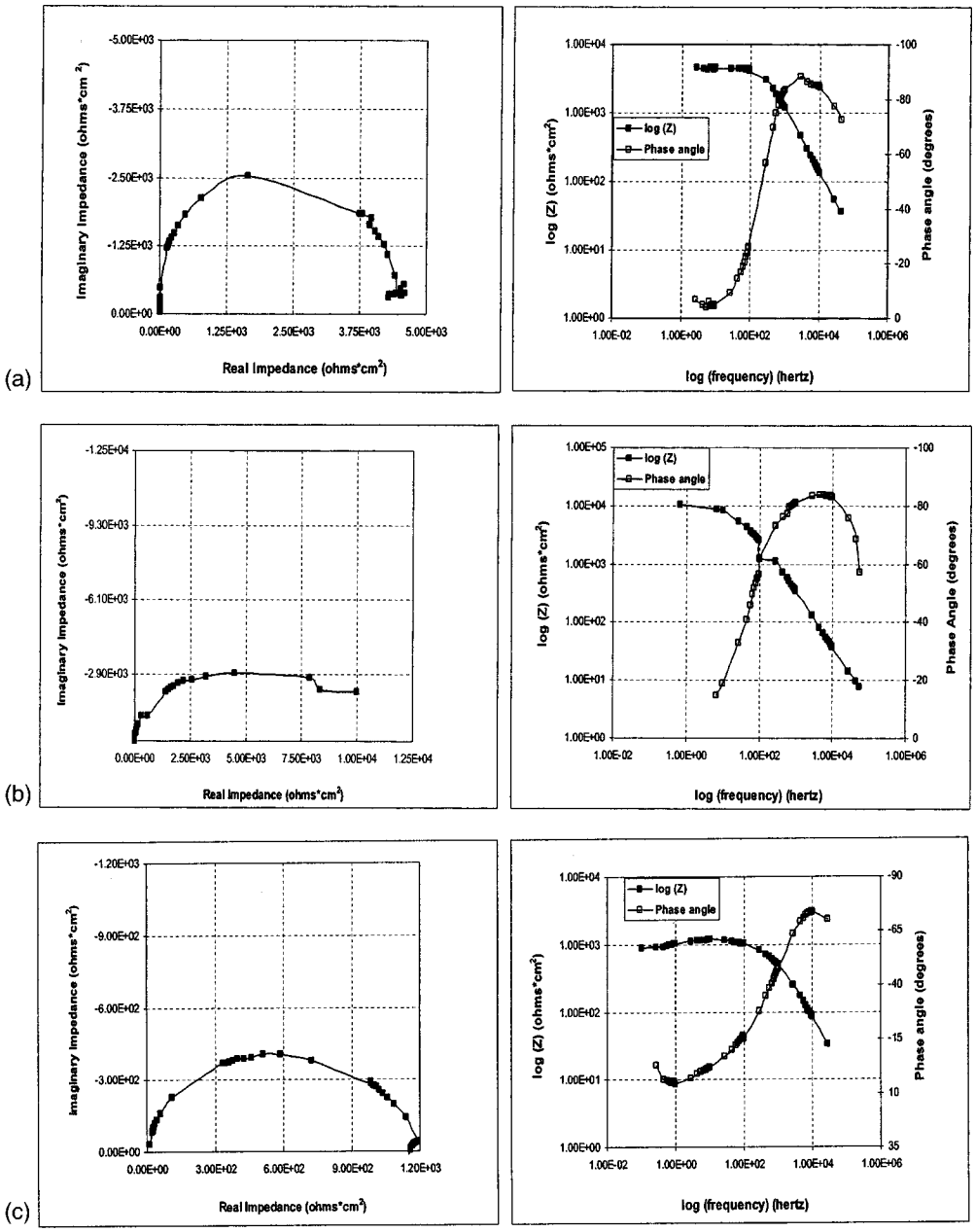

Figure 5. Nyquist and Bode plots of the LEIS response on polyester coil-coated galvanized steel above an area of intact coating after (a) 3 days, (b) 12 days, and (c) 30 days of immersion.

at 1 cm from the defect. Thus, the probe was 40 times the defect diameter away and, at 25 μm from the surface, was 400 times closer to the intact coating than to the defect. Finally, impedance mapping of an area (5000 × 3750 μm) of the specimen including the defect was then carried out at a single frequency of 1 kHz. The probe was moved in the *x* and *y* directions using stepper motors with the probe tip placed 25 ± 1 μm above the sample.

Results

Conventional impedance.—The Nyquist and Bode plots obtained by conventional impedance measurements after 3, 12, 18, and 30 days of immersion are presented in Figures 3a-d, respectively. At shorter immersion times, the response from the macroscopic surface is consistent with a single time constant process plus diffusion. Thus, a solution resistance (R_s) appears in series with a parallel resistor/constant-phase element ($CPE_{coat}//R_{coat}$) related to the properties of the macroscopic surface (*i.e.*, intact coating+defect) with the addition of a limited-layer Warburg diffusional element, $R_{sol} + [CPE_{coat}//(R_{coat} + W_s)]$, where CPE_{coat}, R_{coat} are the generalized, averaged capacitance and resistance of the electrochemically active area (the intact coating plus defect), and W_s is the Warburg impedance. After longer immersion times, the response from the macroscopic surface is consistent with a generalized 2-time constant impedance model for a defective coated surface where a second parallel resistor/constant-phase term ($CPE_{dl}//R_{ct}$), associated with the electrochemistry at the coating defect (charge-transfer resistance and double-layer capacitance, respectively) appears; ($R_{sol} + [CPE_{coat}//(R_{coat} + CPE_{dl}//R_{ct})]$). Thus, with increasing time of immersion, which results in an increased active corrosion area at the defect site, diffusion becomes less important, charge-transfer processes begin to predominate, and the full model is appropriate.

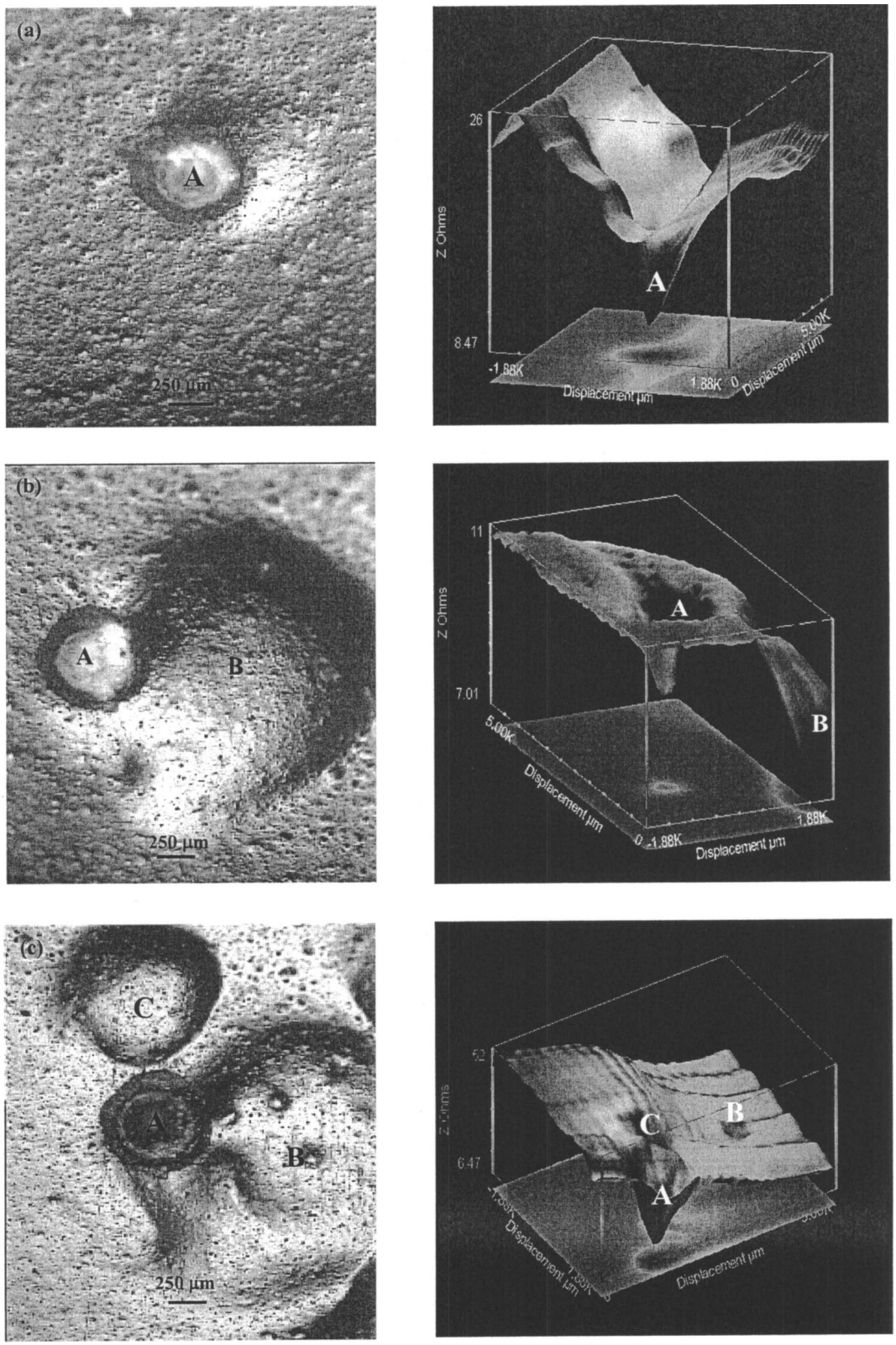

Figure 6. Optical images and corresponding 1 kHz impedance maps of the specimen after (a) 3 days, (b) 18 days, and (c) 30 days of immersion.

LEIS, multifrequency impedance at a single point.—The local impedance response directly above the laser-ablated defect is presented in Fig. 4a-d for 3, 12, 18, and 30 days of immersion, respectively. Here, at shorter immersion times, the LEIS data resemble a single time constant process with diffusion. Thus, after 3 days, a solution resistance (R_s) appears in series with charge transfer ($CPE_{dl}//R_{ct}$) plus a limited-layer (W_s) Warburg, illustrating initial predominant diffusion control (plus charge transfer) at the defect. After 12 days, the low frequency response tends to a capacitive element that is consistent with diffusion through a porous corrosion

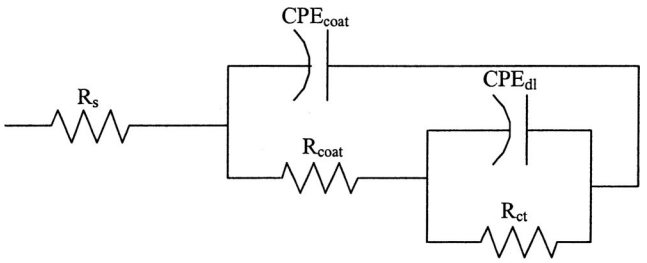

Figure 7. General equivalent circuit fitting the impedance data from the specimen at all days of immersions. R_s represents the solution resistance, R_{coat} is the coating + pore resistance, CPE_{coat} is the coating + pore capacitance, CPE_{dl} is the defect corrosion double-layer capacitance, and R_{ct} is the defect corrosion charge-transfer resistance.

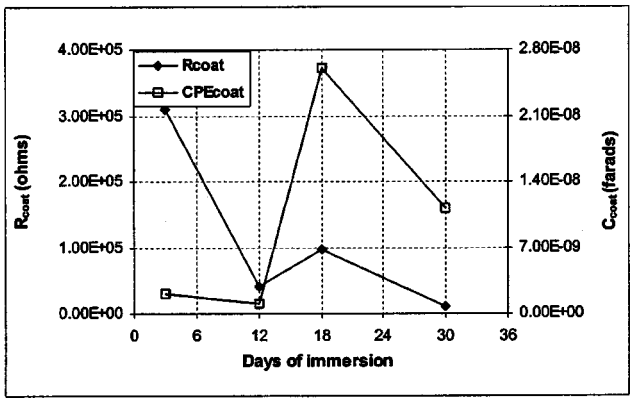

Figure 8. CPE_{coat} and R_{coat} values of the system measured by conventional impedance with immersion time.

product layer. On continuing immersion, the rate-determining step changes to that of predominant charge-transfer control (plus diffusion) after 30 days.

In comparison, the local impedance responses over the intact coating shown in Fig. 5a-c for 3, 12, and 30 days of immersion, are distinctly different from the local responses above the defect. Thus, they reveal only a gradually changing single time constant ($CPE_{coat}//R_{coat}$) in series with the solution resistance (R_s).

LEIS, single frequency impedance mapping.—Maps of the spatial variation in the impedance modulus, $|Z|$, of the sample at 1 kHz after 3, 18, and 30 days of immersion are shown, respectively, in Fig. 6a-c together with corresponding optical micrographs. Note that the vertical scale in Fig. 6 has not been corrected for the constant factor of solution conductivity and probe separation; hence, the units are in ohms. However, the overall trends in the impedance response remain correct. After 3 days, the defect is evident at point A on the micrograph, and this is reflected in the impedance map as a large decrease in $|Z|$ localized at the defect. After 18 days, significant underfilm corrosion has initiated, and this is again evident in the impedance map as a reduction in $|Z|$ coinciding with the visible damage in the optical image (point B in the image). After 30 days of immersion, the original area of underfilm corrosion has started to blister, and this again coincides with a substantial decrease in local $|Z|$ centered at the defect and visible in the modulus map.

Discussion

General equivalent circuit impedance model.—The proposed generalized equivalent circuit, which is consistent with all the impedance data, is shown in Fig. 7. Here, R_s represents the solution resistance of the electrolyte. The first time constant is represented by a constant-phase element (CPE_{coat}) in parallel with a resistance (R_{coat}) and is conventionally associated with the generalized macroscopic properties of the coating plus the defect. The second time constant (R_{ct}/CPE_{dl}) conventionally represents electrochemical processes at the defect (and may be replaced by a limited-layer Warburg impedance, W_s, in the event of significant diffusional control).

Conventional macroscopic impedance.—At 3 days immersion, Fig. 3a, the impedance model can be represented essentially by a single time constant process with diffusion. Thus, at the pre-existing defect, penetration of the electrolyte underneath the coating leads to an increasing area of corrosion on the substrate and disbonding of the coating. As the corrosion spreads, it is suggested that a film of corrosion products blocks the defect, slowing the entrance of electrochemically active species. This causes a diffusion process, which is represented by a Warburg element (*i.e.*, replacing (R_{ct}/CPE_{dl}) in the equivalent circuit of Fig. 7).

From 12 to 30 days immersion, Fig. 3b-d, the impedance data from the macroscopic surface features two time constants and is consistent with the equivalent circuit of Fig. 7. The higher frequency process, similar to that observed after 3 days, represents the macroscopic coating + defect properties (R_{coat}/CPE_{coat}). The lower frequency time constant (R_{ct}/CPE_{dl}) represents the double layer formed by the metal/electrolyte interface and corresponds to corrosion processes (both anodic and cathodic) occurring at the base of the defect and under the coating. Figure 8 shows how the resistance and capacitance evolve with time for the first time constant of the system (*i.e.*, corresponding to the macroscopic coating + defect properties).

The macroscopic coating + defect resistance initially drops between 3 and 12 days immersion, while the capacitance shows little variation (a slight drop). There are significant increases in the values of resistance and capacitance between 12 and 18 days with a subsequent decrease in both parameters from 18 to 30 days immersion.

Such behavior is conventionally explained by consideration of the changes in water content of the coating and any corrosion processes occurring at the defect. Thus, in the intact (perfect) regions of the coating, water uptake into the coating is expected to decrease coating resistance (water has a higher bulk conductivity compared with typical polymers) but increase coating capacitance (water has a higher dielectric constant compared with typical polymers). However, at the defect, as corrosion products build up, transient pore plugging may occur leading to a large area of relatively conductive corrosion product with a consequent increased resistance (due to a protective effect) and increased capacitance (due to the active area). After 18 days, as additional active sites and blisters develop (Fig. 6), the importance of film blocking and diffusion as the rate-determining process decreases relative to that of the charge-transfer (active corrosion) reaction.

The evolution with time of the parameters from the second time constant of the conventional impedance data is shown in Fig. 9. These show a steadily increasing double layer capacitance with time from 12 to 30 days immersion and a corresponding decrease in charge resistance with time. These features conventionally correspond to a progressive increase in the corroded area with time.

LEIS, multifrequency single point.—Local electrochemical impedance permits, in principle, the measurement of an impedance response from a limited area of a surface rather than over the whole macroscopic surface. This is clearly illustrated by the substantially different local impedance response from the defect area (Fig. 4) and over an area of intact coating (Fig. 5). In the former case, after 3 and 12 days immersion, the relevant impedance model is essentially a single time constant (charge-transfer) process plus diffusion. Thus, the charge-transfer impedance clearly represents the corrosion process directly, with the Warburg impedance representing diffusion of

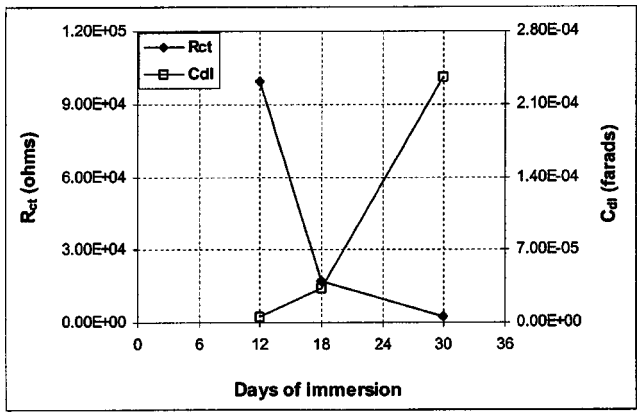

Figure 9. CPE_{dl} and R_{ct} values evolution of the system measured by conventional impedance with immersion time.

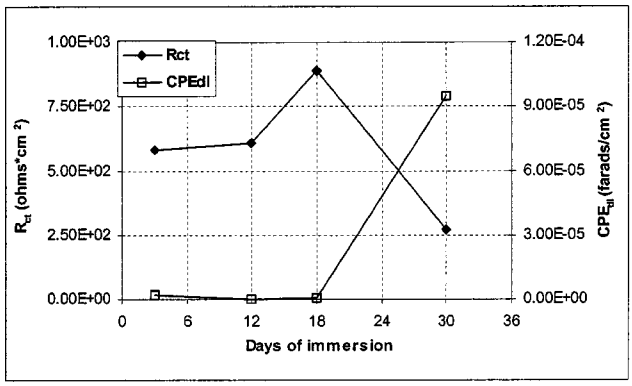

Figure 10. Evolution of the CPE_{dl} and R_{ct} values of LEIS data over the coating defect with immersion time.

active species through a plug of corrosion product at the defect. The evolution of R_{ct} and CPE_{dl} with increasing time of immersion is shown in Fig. 10. Up to 18 days, there is a gradual increase in charge-transfer resistance, presumably due to increased pore blockage with corrosion product. After 18 days, the charge-transfer resistance decreases substantially with a corresponding increase in capacitance as the additional areas of active blistering develop (see Fig. 6).

Figure 5a-c displays the Nyquist and Bode plots for LEIS above the coating from 3 to 30 days of immersion. Here, for all immersion periods, a single time constant is observed which clearly corresponds directly to the capacitance and resistance of the coating (R_{coat} and CPE_{coat}) with the terms in the second time constant of the equivalent circuit model (Fig. 7) set to zero. Figure 11 shows the evolution in the values of R_{coat} and CPE_{coat} with time for the intact area of the coating. After an initial rise, the coating resistance shows a large decrease with time. Significantly, the measured coating capacitance increases steadily with time consistent with increasing water uptake into the polymer.

Impedance mapping.—Figures 6a-c show maps of the impedance modulus over the specimen from 3 to 30 days of exposure in 10 mM NaCl. Optical images of the sample, taken on the same day, are displayed alongside. The defect area A in the coating corresponds identically to the lowest value of modulus in the impedance map. Obviously, the mapping technique demonstrates the lowest resistance ($|Z|$) in the area of the laser-ablated hole when compared to the coated surface. After 18 days of immersion, zone B corresponds to a second area of low impedance and correlates to the optical image by the formation of a blister next to the laser defect. After 30 days of immersion, three areas of low impedance are evident. The lowest modulus still corresponds to the area of the coating defect, zone A, and may be compared with the laser hole on the optical image. Zone B has a much larger area than at 18 days, starting from the edge of the holiday and extending to its right side. The third region corresponds to a well-defined area of lower impedance within zone B, which corresponds to a blister on the optical image. These blistered zones are formed around the original defect and are generated by the underfilm corrosion beginning at the exposed metal in the laser-created holiday. They are clearly seen optically and by LEIS mapping, and, as demonstrated previously, multifrequency LEIS over a single point can provide detailed information about the local performance of the coating at that point.

Comparing macroscopic EIS with single point LEIS and LEIS mapping.—The macroscopic EIS and the two local LEIS measurements are directly comparable as they were obtained from the same samples in the same environment at the same locations and within a few hours of each other. The LEIS data, which were obtained directly over the intact coating, clearly demonstrate the theoretical single time constant process due to a parallel plate capacitor comprised of the metal substrate and electrolyte, separated by the coating dielectric. The trends from this data (Fig. 11) closely follow those expected from water uptake into a free dielectric film. Thus, significantly, there appears to be no interference from Faradaic (corrosion) processes in defect areas.

However, significant differences are evident between the LEIS data for the intact coating and the first time constant process (usually associated with coating properties) obtained using conventional EIS. In particular, the EIS capacitance data (CPE_{coat}) do not show a steady increase with time and are clearly convoluted in some way with the impedance response from the defect. Similarly, the trend in the LEIS data from above the defect is essentially as expected for a bare corroding metal where the surface is occluded by a corrosion product for a time and then the area of corrosion increases due to blistering and underfilm corrosion. However, the EIS data from the second time constant process (conventionally associated solely with the corrosion reaction at the defect) shows a different trend with a steadily decreasing resistance and increasing capacitance.

In reconciling these differences, we point out that great care was taken to ensure a true local impedance measurement. Thus, in most previously reported LEIS methods, despite the current being determined locally, the potential is measured remotely and thus is an average over the surface. This is likely to contribute significant errors or artifacts to the notional LEIS measurement. However, we use a novel form of LEIS measurement, where, in addition to determining the local current density by a dual electrode, the local potential adjacent to the surface is also directly determined. Hence, the measurement is more likely to reflect the true local impedance.

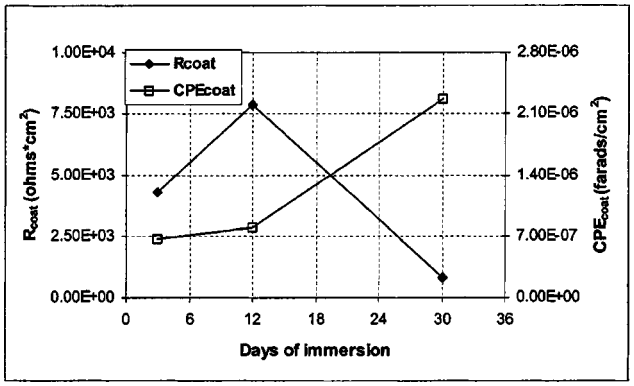

Figure 11. Evolution of the CPE_{coat} and R_{coat} values of LEIS data from the area of intact coating with immersion time.

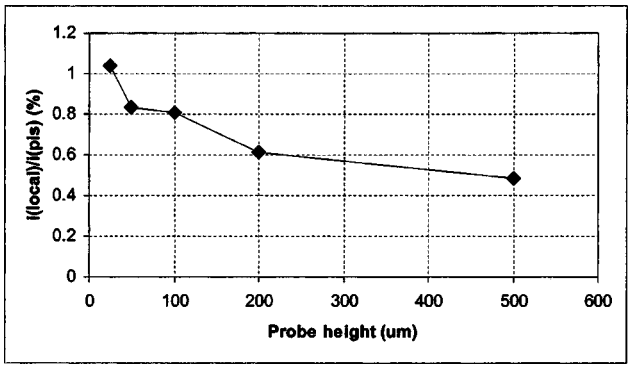

Figure 12. Chart showing the percentage current sensed by the LEIS probe using a point-in-space calibration electrode.

Comparison of Fig. 8 with Fig. 11 shows that the EIS impedance is approximately 100 times larger than the LEIS impedance. This magnitude difference occurs primarily because the LEIS probe only captures a small fraction of the local current density emerging at the defect. Hence, in Eq. 2, if the local current is less than its correct value, the impedance is also too small by the same quantity. To determine the correction factor, the local current captured by the probe was measured in equimolar Fe(II)/Fe(III) (to provide a stable redox potential for the platinum probes) using a point-in-space electrode of the same diameter as the defect (250 μm). Figure 12 reports a calibration chart of the percentage current captured by the LEIS probe, which shows that, at the probe working distance of 25 μm, approximately 1% of the local current density is sensed. Hence, the true LEIS impedance values should be multiplied by 100. This correction brings the two sets of data (EIS and LEIS) within the same order of magnitude.

Given that we believe the LEIS data reported here to be correct, we must determine that the two time constants evident in the macroscopic EIS measurement do not represent distinct and separable physical processes and that the data are, therefore, convoluted together. This implies that great care should be exercised in the physical interpretation of conventional impedance data from defectively coated surfaces. Ideally, separate local impedance measurements must be performed to properly distinguish the true coating response from the true defect response.

Conclusions

1. Traditional (EIS) and localized impedance spectroscopy (LEIS) have been used to study the solution degradation of an organic coating with a laser-ablated artificial defect. The LEIS results clearly demonstrate that it is possible to separate the impedance response of the intact coating from that of the defect. In addition, single frequency impedance mapping of the surface can provide complementary data supporting the physical interpretations of the impedance response.

2. In this work, the traditional macroscopic EIS data reveal two time constants that are conventionally associated with separate coating and defect processes. However, comparison of the trends of derived resistance and capacitance values as a function of time with corresponding LEIS data obtained separately from the intact coating and the defect strongly imply that the EIS data cannot be represented as separate processes within distinct time domains. Thus, the coating and defect processes appear to be convoluted together.

3. Great care must be taken in interpreting conventional EIS data using an equivalent circuit representation. It is clear from the LEIS data presented here that, although two distinct time constants in the EIS data may appear, the physical processes associated with the overall response are not necessarily separable into two time domains. Thus, resistance and capacitance parameters extracted from such an interpretation are likely to represent an average response rather than a true response.

University of Manchester Institute of Science and Technology assisted in meeting the publication costs of this article.

References

1. C. H. Hare, *Fed. Soc. Coat. Techno.*, **53**, 29 (1981).
2. D. Y. Perera and P. Selier, *Prog. Org. Coat.*, **1**, 57 (1973).
3. P. Walker, *J. Paint Technol.*, **37**, 102 (1967).
4. H. Leidheiser, *Corrosion (Houston)*, **38**, 374 (1982).
5. H. Leidheiser, in *Polymeric Materials for Corrosion Control*, R. A. Dickie and F. L. Floyd, Editors, *Symposium Series, American Chemical Society*, p. 124 (1986).
6. J. S. Thornton, J. F. Cartier, and R. W. Thomas, in *Polymeric Materials for Corrosion Control*, R. A. Dickie and F. L. Floyd, Editors. Symposium Series, American Chemical Society, p. 169 (1986).
7. D. H. van der Weidje, E. P. M. van Westing, and J. W. H. der Wit, *Electrochim. Acta*, **41**, 1103 (1996).
8. E. L. Koehler, in *Localized Corrosion*, R. W. Staehle, B. F. Brown, J. Kruger, and A. Agrawal, Editors, p. 117, NACE, Houston, TX (1974).
9. G. M. Hogh, in *Localized Corrosion*, R. W. Staehle, B. F. Brown, J. Kruger, and A. Agrawal, Editors, p. 134, NACE, Houston, TX (1974).
10. G. Grundmeier, W. Schmidt, and M. Stratmann, *Electrochim. Acta*, **45**, 2515 (2000).
11. G. W. Walter, *Corros. Sci.*, **26**, 681 (1986).
12. F. Mansfeld, *Electrochim. Acta*, **35**, 1533 (1990).
13. H. S. Isaacs and M. W. Kending, *Corrosion (Houston)*, **36**, 269 (1980).
14. J. V. Standish and H. Leidheiser, *Corrosion (Houston)*, **36**, 390 (1980).
15. M. C. Hughes and J. M. Parks, *Corrosion Control by Organic Coatings*, H. Leidheiser, Jr., Editor, p. 45, NACE, Houston, TX (1981).
16. R. S. Lillard, P. J. Moran, and H. S. Isaacs, *J. Electrochem. Soc.*, **139**, 1007 (1992).
17. M. W. Wittman and S. R. Taylor, in *Advances in Corrosion Prevention by Organic Coatings II*, M. W. Kendig and J. D. Scantlebury, Editors, PV 95-13, p. 158, The Electrochemical Society Proceedings Series, Pennington, NJ (1995).
18. F. Zou and D. Thierry, *Electrochim. Acta*, **42**, 3293 (1997).